Rational design and syntheses of 0-D, 1-D, and 2-D metal-organic frameworks (MOFs) from ferrocenedicarboxylate tetrametallic macrocyclic building units and subsidiary ligands

Liping Wang, Xiangru Meng, Erpeng Zhang, Hongwei Hou *, Yaoting Fan

Department of Chemistry, Zhengzhou University, Zhengzhou, Henan 450052, PR China

Abstract

We have designed and synthesized three new metal-1,1′-ferrocenedicarboxylate complexes containing tetrametallic macrocyclic building units, namely, $[Cd_2(\eta^2-O_2CFcCO_2-\eta^2)_2(phen)_2(H_2O)_2] \cdot 4CH_3OH$ (1) ($Fc = (\eta^5-C_5H_4)Fe(C_5H_4-\eta^5)$, phen = 1,10-phenanthroline), $\{[Cd(\eta^2-O_2CFcCO_2)(pebbm)(H_2O)] \cdot 2H_2O\}_n$ (2) (pebbm = 1,1′-(1,5-pentanediyl)bis-1H-benzimidazole) and $\{[Cd(\eta^2-O_2CFcCO_2-\eta^2)-(prbbm)(H_2O)] \cdot 3H_2O\}_n$ (3) (prbbm = 1,1′-(1,3-propanediyl)bis-1H-benzimidazole). Compound 1 is a 0-D discrete tetrametallic macrocyclic framework. Compound 2 features an infinite 1-D ribbon of rings structure constructed by the subsidiary ligands pebbm connecting tetrametallic macrocyclic building units. For 3, its tetrametallic macrocyclic building units are linked by the subsidiary ligands prbbm to form a 2-D network structure. The structural features of these complexes indicate that the ferrocenedicarboxylate tetrametallic macrocycle can be used as a successful molecular building unit and the shapes and conformational flexibility of subsidiary ligands play a crucial role in the manipulation of the configuration of the resultant MOFs. Their fluorescence spectra in solid state at room temperature suggest that the fluorescence emissions of 1–3 are ruled by 1,1′-ferrocenedicarboxylate ligand.
© 2007 Published by Elsevier B.V.

Keywords: Metal-organic frameworks (MOFs); Sodium 1,1′-ferrocenedicarboxylate; Subsidiary ligands; Tetrametallic macrocyclic building units; Luminescence properties

1. Introduction

In recent years, the rational design and syntheses of discrete or extended metal-organic frameworks (MOFs) have been extensively explored for their versatile molecular architectures and topologies as well as their great potential applications as multifunctional materials [1]. At the same time, considerable progress have been made on the theoretical forecast and practical approaches [2], but in many cases the control of the configuration of MOFs is a major challenge in a truly deliberate manner, due to the influence of various factors, such as the coordination geometry of the central metal ion, the flexibility and shape of the organic ligand, metal–ligand ratio, PH value [1b,3].

In order to control the structures of MOFs effectively, many attempts have been made and the manner of rational utilization of molecular building units including "preprogrammed" structural information has been proved to be an efficient strategy [4]. In the reported literatures, the most successful molecular building units used in the construction of MOFs is the paddle wheel dinuclear unit $M_2(CO_2)_4$ formed by four carboxylate anions bridging two metal ions (Scheme 1a) [5]. Such units can be regarded as nodes, and multifunctional organic ligands link these nodes resulting in diverse MOFs that vary from discrete molecules to infinite networks [1a]. Recently, many other conformations of molecular building units have also been reported, such as triangular, tetrahedral, trigonal prismatic, octahedral and planar tetracopper molecular building units [3a,6].
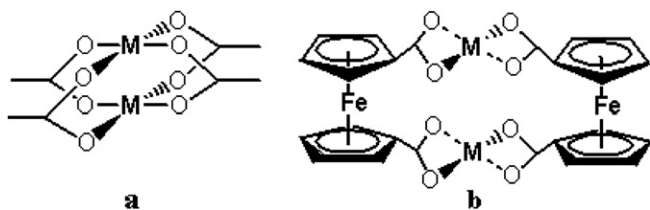
Scheme 1.

The elaborate selection of suitable organic ligands is of particular importance in engendering MOFs with desirable dimension, because it is likely to control the distance between the metals and hence control the dimensions of the resultant aggregates [7]. For instance, tailored derivatives of 4,4-bipyridine ligands with various spacers between two pyridine groups have been proved to be excellent candidates to control the dimensionality of metal-organic frameworks [3c,8]. In general, rigid organic ligands may allow a controllable growth of the crystal structure, in contrast, flexible organic ligands, for some factors such as the length and conformational flexibility as well as the rotational freedom of the heterocycle rings, usually bring on structural diversification of the products, including the formation of supramolecular isomers [7b,8a,9]. In summary, through rational design of building units and organic ligands, structures of the MOFs can be controlled or predicted.

With this background, our group has recently started on a program aimed at designing new MOFs by rational utilization of molecular building units including "preprogrammed" structural information and functional organometallic groups, as well as elaborate selection of subsidiary organic ligands. In this paper, we find that 1,1′-ferrocenedicarboxylate tetrametallic macrocyclic unit (Scheme 1b) can act as a good molecular building unit. Through the introduction of suitable subsidiary organic ligands, three new complexes, namely, 0-D discrete tetrametallic macrocyclic framework complex $[Cd_2(\eta^2-O_2CFcCO_2-\eta^2)_2(phen)_2(H_2O)_2] \cdot 4CH_3OH$ (**1**), 1-D ribbon of rings complex $\{[Cd(\eta^2-O_2CFcCO_2)(pebbm)(H_2O)] \cdot 2H_2O\}_n$ (**2**) and 2-D network complex $\{[Cd(\eta^2-O_2CFcCO_2-\eta^2)(prbbm)(H_2O)] \cdot 3H_2O\}_n$ (**3**), have been successfully obtained (Scheme 2). Furthermore, the fluorescence properties of complexes **1–3** and sodium 1,1′-ferrocenedicarboxylate are investigated in solid state at room temperature.
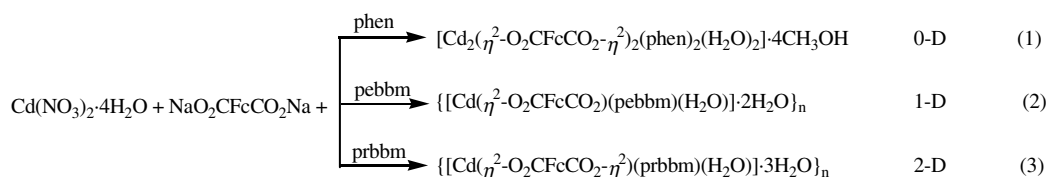
2. Results and discussion

2.1. Design of the complexes

As well known, 1,1′-ferrocenedicarboxylate as a very important multifunctional ligand has attracted much attention owing to the size and the strong inductive effect of ferrocene as well as the versatile coordination modes of carboxylate anions [10–24]. Among the reported metal-1,1′-ferrocenedicarboxylate complexes, we found several complexes containing similar tetrametallic macrocyclic units, such as $[M_2(\eta^2-O_2CFcCO_2)_2(2,2′-bpy)_2(H_2O)_2]$ (M = Zn; Cd) [19], $[Zn(O_2CFcCO_2)(1-methylimidazole)_2]_2$ [20], and $[Cu(O_2CFcCO_2)(Py)(DMF)(H_2O)]_2$ [21]. These tetrametallic macrocyclic units (show in Scheme 1b) are all formed by virtue of two 1,1′-ferrocenedicarboxylate anions bridging two divalent metal ions, though the coordination modes of carboxylate groups have little difference. It is worthy to note that the two divalent metal ions in every tetrametallic macrocyclic unit are coordinatively unsaturated. This indicates that the tetrametallic macrocyclic unit can be used as a molecular building unit with "preprogrammed" structural information. When subsidiary ligands with different shapes and conformations combine with the coordinatively unsaturated metal ions, multifarious MOFs containing such tetrametallic macrocyclic units can be constructed. According to this idea, we introduce a chelating ligand phen to the tetrametallic macrocyclic units constructed by $Cd(NO_3)_2 \cdot 4H_2O$ and 1,1′-ferrocenedicarboxylate and obtain one 0-D complex **1** successfully. Analogously, an infinite 1-D ribbon of rings complex **2** or a 2-D network complex **3** can be generated by introducing bridging ligands such as pebbm or prbbm to the tetrametallic macrocyclic units. To the best of our knowledge, the infinite extended coordination polymers containing 1,1′-ferrocenedicarboxylate tetrametallic macrocyclic units are still very rare [22].

2.2. Description of crystal structures

Single crystal X-ray determination suggests that **1** is a 0-D discrete dimer in which there is a tetrametallic macrocyclic unit formed by two 1,1′-ferrocenedicarboxylate anions bridging two Cd(II) ions (Fig. 1a and b). Each Cd(II) ion is seven coordinated by two nitrogen atoms from one chelating phen ligand and five oxygen atoms from two 1,1′-ferrocenedicarboxylate groups and one water molecule. There

$Cd(NO_3)_2 \cdot 4H_2O + NaO_2CFcCO_2Na +$

phen → $[Cd_2(\eta^2-O_2CFcCO_2-\eta^2)_2(phen)_2(H_2O)_2] \cdot 4CH_3OH$ 0-D   (1)

pebbm → $\{[Cd(\eta^2-O_2CFcCO_2)(pebbm)(H_2O)] \cdot 2H_2O\}_n$ 1-D   (2)

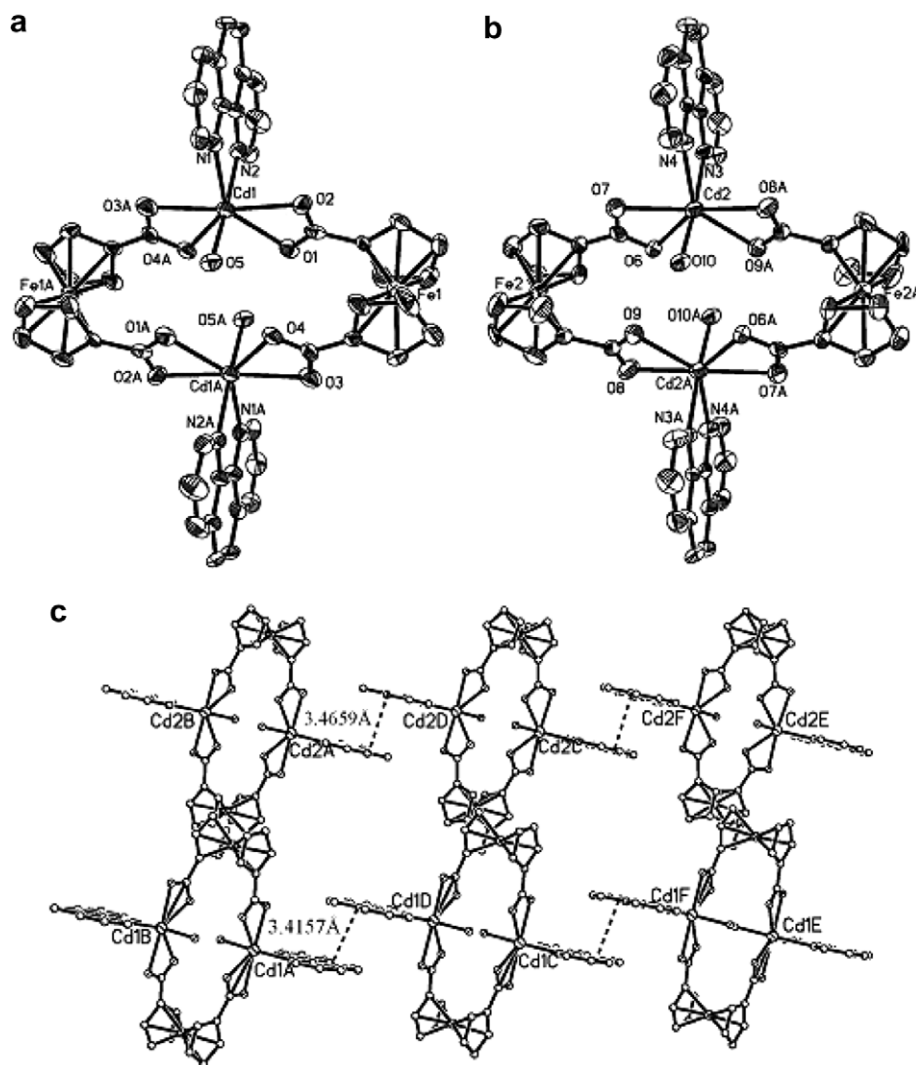prbbm → $\{[Cd(\eta^2-O_2CFcCO_2-\eta^2)(prbbm)(H_2O)] \cdot 3H_2O\}_n$ 2-D   (3)

Scheme 2.

Fig. 1. (a) Perspective drawing of $Cd(1)_2(\eta^2\text{-}O_2CFcCO_2\text{-}\eta^2)_2(phen)_2(H_2O)_2$ groups in complex **1**. (b) Perspective drawing of $Cd(2)_2(\eta^2\text{-}O_2CFcCO_2\text{-}\eta^2)_2(phen)_2(H_2O)_2$ groups in complex **1**. (c) View of 1-D chain in complex **1** showing the π–π interactions between the phen rings. The hydrogen atoms and uncoordinated methanol molecules are omitted for clarity in (a), (b) and (c).

are two crystallographically independent Cd(II) ions (Cd1 and Cd2). Around Cd1 (Fig. 1a), O1, O2, O3A, O4A and N1 atoms occupy the equatorial positions, while O5, N2 are in axial positions, so the local coordination environment of Cd1 can be described as a distorted pentagonal bipyramid. Two Cd1–N bond lengths are 2.344(7) and 2.366(8) Å, five Cd1–O bond lengths are 2.385(7), 2.474(7), 2.426(8), 2.400(6) and 2.331(6) Å, respectively. Meanwhile, the four co-planar metal ions Cd1, Cd1A, Fe1, and Fe1A (the mean deviation from plane is 0.0000 Å) form a rhombus with the side lengths of 5.705 and 5.697 Å and the interior angles of 52.05° and 127.95°, respectively. The coordination geometry of Cd2 is similar to that of Cd1 (Fig. 1b), only the corresponding bond lengths and angles have slightly differences. Detailed data of bond lengths and angles around Cd2 are shown in Table 2.

The phen rings between adjacent $Cd(1)_2(\eta^2\text{-}O_2CFcCO_2\text{-}\eta^2)_2(phen)_2(H_2O)_2$ groups or $Cd(2)_2(\eta^2\text{-}O_2CFcCO_2\text{-}\eta^2)_2(phen)_2(H_2O)_2$ units are parallel with the

average interplanar distance of 3.4125 or 3.4691 Å, which is in the range of common distances for π–π interactions between two aryl rings [19,25–27]. These π–π interactions among phen rings link the discrete tetrametallic macrocyclic units resulting in a 1-D infinite chain, as show in Fig. 1c. Although the π–π interactions are weak, these kinds of interactions are important in the molecular assembly.

The crystal structure of **2** is significantly different from **1**; it displays an interesting infinite 1-D ribbon of rings structure composed of two kinds of rings, the smaller 16-membered ring and the larger 24-membered ring (Fig. 2b). The smaller ring is a tetrametallic macrocyclic unit, in which two Cd(II) ions and two Fe(II) ions also form a rhombus (similar to that of **1**) with the sides of 5.594 and 5.772 Å, the interior angles of 56.13° and 123.87°, and the Cd(II)$\cdots$Cd(II) distance of 5.350 Å. The larger ring is formed by two pebbm molecules bridging two Cd(II) ions and the Cd(II)$\cdots$Cd(II) distance is 14.403 Å. The above two kinds of rings are
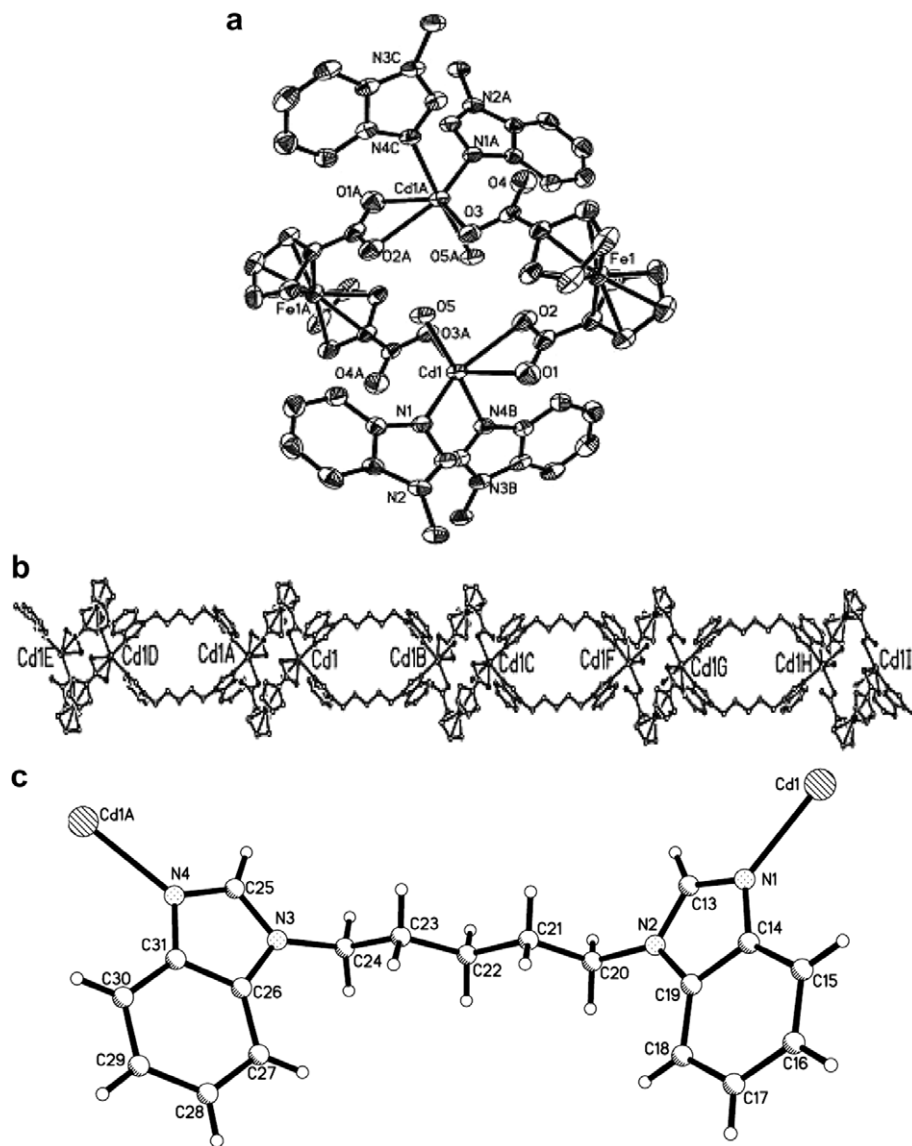
Fig. 2. (a) The tetrametallic macrocyclic unit in complex **2**. (b) Perspective drawing of complex **2** showing 1-D ribbon of rings framework. (c) Perspective view showing the contents of the pebbm unit and the connected atoms in the crystal structure of **2**. The hydrogen atoms and uncoordinated water molecules are omitted for clarity in (a) and (b).

connected alternately *via* Cd(II) ions forming an infinite 1-D chain.

In complex **2**, all of the Cd(II) ions, the 1,1′-ferrocenedicarboxylate groups and the pebbm ligands are equivalent, respectively. Each Cd(II) ion is coordinated by six donors: two nitrogen atoms from two bridging pebbm molecules, three oxygen atoms belonging to two 1,1′-ferrocenedicarboxylate groups and one oxygen atom from coordination water molecule (Fig. 2a). O1, O2, O3A and N1 atoms occupy the equatorial positions and O5, N4B are in axial positions, which results in distorted octahedron geometry. Around the Cd(II) ion, the Cd–N bond lengths are 2.300(2) and 2.353(3) Å, and the Cd–O bond lengths are in the range of 2.282(2)–2.498(2) Å.

As shown in Fig. 3b, complex **3** displays a particular 2-D network framework constructed by prbbm ligands bridging

the tetrametallic macrocyclic units. The configuration of the tetrametallic macrocyclic unit in **3** is different from that in **2**, but nearly identical to that in **1** excluding slight differences in the corresponding bond lengths and bond angles. The four metal ions (Cd1, Cd1A, Fe1, and Fe1A) in each tetrametallic macrocyclic unit also form a rhombus with the sides of 5.632 and 5.667 Å and the interior angles of 56.76° and 123.24°, respectively (Fig. 3a). Each Cd(II) ion is located in an analogical distorted pentagonal bipyramid as that in **1**. Around Cd(II) ion, seven coordination atoms are two nitrogen atoms from two bridging ligands and five oxygen atoms from two 1,1′-ferrocenedicarboxylate groups and one water molecule. Among them, O1, O2, O3A, O4A and N1 atoms occupy the equatorial positions, while O5, N4B are in axial positions. Two Cd1–N bond lengths are 2.271(4) and 2.310(4) Å, the
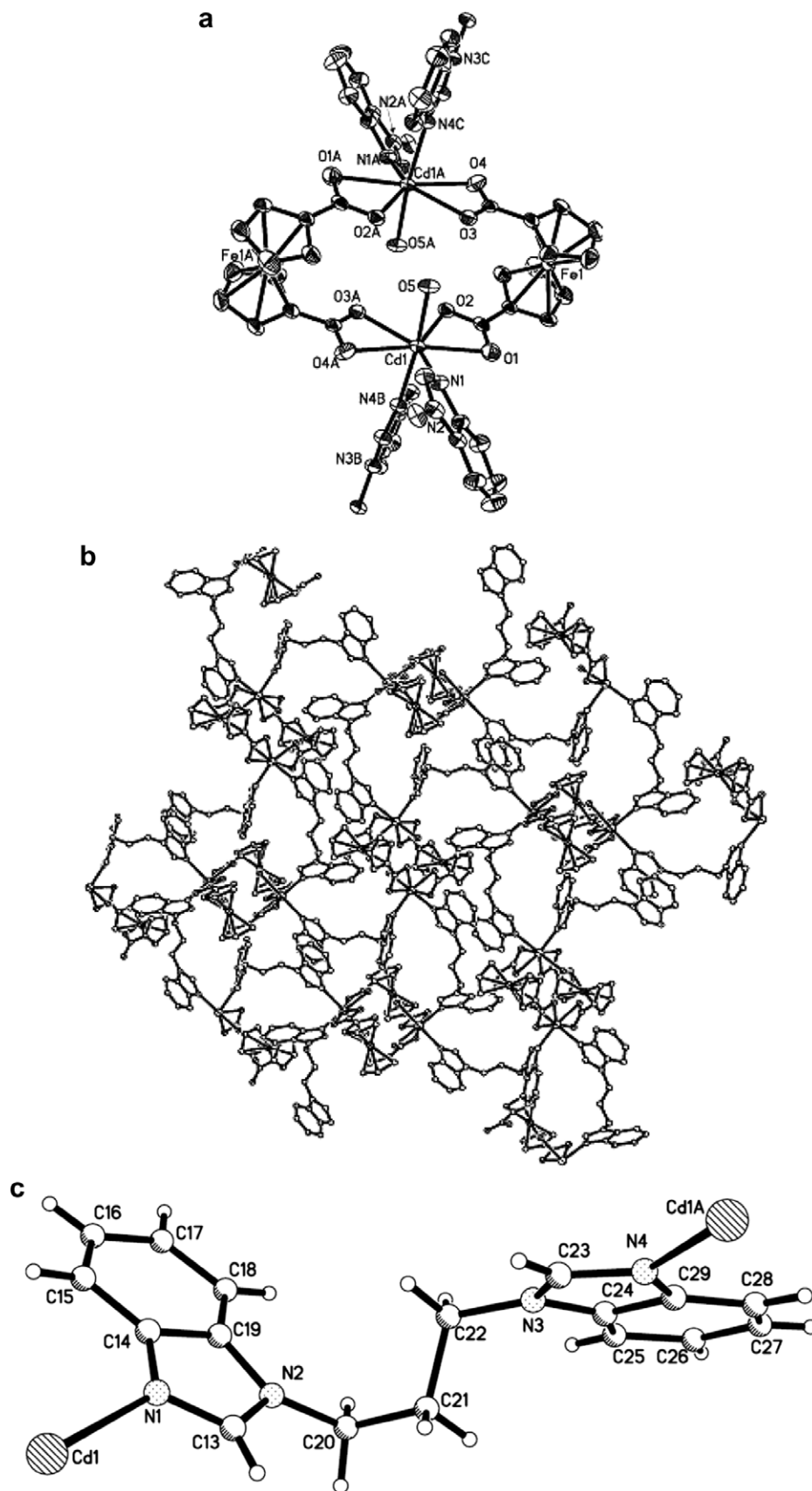
Fig. 3. (a) The tetrametallic macrocyclic unit in complex **3**. (b) Perspective drawing of complex **3** showing 2-D network framework. (c) Perspective view showing the contents of the prbbm unit and the connected atoms in the crystal structure of **3**. The hydrogen atoms and uncoordinated water molecules are omitted for clarity in (a) and (b).

Cd–O bond lengths are in the range of 2.295(4)–2.616(4) Å, which are close to those in **1**.

It should be noted that there are few dissimilarities in the 1,1′-ferrocenedicarboxylate tetrametallic macrocyclic units among the complexes containing this unit. The coordination modes of the two carboxylate groups of 1,1′-ferrocenedicarboxylate in **1** and **3** are both bidentate-chelation, which have not been reported yet. However, in the case of **2**, one carboxylate group of 1,1′-ferrocenedicarboxylate is bidentate-chelating mode, another carboxylate group is mono-dentate fashion, and the same coordination fashion can be found in $[M_2(\eta^2\text{-}O_2CFcCO_2)_2$ $(2,2'\text{-bpy})_2(H_2O)_2]$ (M = Zn; Cd) [19]. In addition, two carboxylate groups of 1,1′-ferrocenedicarboxylate can also adopt mono-dentate fashion at the same time, as observed in $[Zn(O_2CFcCO_2)\text{-}(1\text{-methylimidazole})_2]_2$ [20] and $[Cu(O_2CFcCO_2)(Py)\text{-}(DMF)(H_2O)]_2$ [21].

2.3. Discussion

As far as we know, although 1,1′-ferrocenedicarboxylate tetrametallic macrocyclic unit has been reported [19–21], here it is used purposefully as a molecular building unit for the first time, and the experiment results prove that our ideas are successful. Different from other familiar molecular building units, 1,1′-ferrocenedicarboxylate tetrametallic macrocyclic unit combine functional organometallic-ferrocene group into molecular building unit and can provides an effective way to prepare new functional MOFs with unusual properties. Further investigations of those complexes containing 1,1′-ferrocenedicarboxylate tetrametallic macrocyclic units indicate that the differences of the shapes and conformational flexibility of subsidiary ligands leads to different structures of the resultant MOFs. Concretely, the terminal monodentate ligands like py, or chelating ligands like phen and 2,2′-bpy, are capable of "passivate" metal sites, which induces 0-D discrete tetrametallic macrocyclic frameworks, such as $[M_2(\eta^2\text{-}O_2CFcCO_2)_2(2,2'\text{-bpy})_2(H_2O)_2]$ (M = Zn; Cd) [19], $[Zn(O_2CFcCO_2)(1\text{-methylimidazole})_2]_2$ [20], $[Cu(O_2CFcCO_2)(Py)(DMF)(H_2O)]_2$ [21] and complex **1**. The bridging ligands, such as pebbm and prbbm, can be acted as the bridges, which lead to the infinite extended coordination polymers, such as **2** and **3**. However, the structures of **2** and **3** are completely different although they contain similar bridging ligands. One factor should be ascribed to the different lengths of the pebbm and prbbm ligands, which result in the unequal Cd···Cd distances and then the distinct structures of **2** and **3**. The other can be explained by the different conformational flexibility between the pebbm and prbbm ligands. To our knowledge, the various conformational flexibilities of ligand usually lead to great structural diversification of the products [7b–9]. For example, many coordination polymers containing the flexible ligand bpp have multifarious-dimensional structures because the bpp molecule [1,3-bis(4-pyridyl)propane] can adopt TT, TG, GG, and GG′ conformations (where T = *trans* and

G = *gauche*) [9e–j]. In our paper, the pebbm in **2** adopts TTTT conformation [the torsional angles of the fragments of C19–N2–C20–C21, N2–C20–C21–C22, C20–C21–C22–C23, C21–C22–C23–C24, C22–C23–C24–N3 and C26–N3–C24–C23 are 86.2(4)°, 177.6(3)°, 177.0(3)°, 176.2(3)°, 172.0(3)° and −79.0(4)°, respectively] (Fig. 2c). As a result, two pebbm molecules with this conformation manner are inclined to link two Cd(II) ions simultaneously, which conduce the formation of the double-bridge and thereby bring on the 1-D chain structure. Whereas in **3**, prbbm adopts TG conformation [the torsional angles of the fragments of C19–N2–C20–C21, N2–C20–C21–C22, C20–C21–C22–N3 and C24–N3–C22–C21 are 115.2(6)°, −69.1(7)°, −174.8(5)° and 79.8(6)°] as show in Fig. 3c. This implies that the relative orientation of the two benzimidazole groups of prbbm in **3** is different from that of pebbm in **2**. Such prbbm groups can be propagated in two directions and in this way a 2-D network arises. In a word, the length and especially the conformational flexibility of alkyl spacers as well as the rotational freedom of the benzimidazole rings observed in the auxiliary ligands, is responsible for the relative orientations of N donor atoms, which leads to the different structures of **2** and **3**.

The structural features of complexes **1–3** suggested that 1,1′-ferrocenedicarboxylate tetrametallic macrocycle can be used as a successful molecular building unit in the construction of predictable MOFs, and more fascinating coordination polymeric frameworks will be rationally designed by the assembly of metal ions and 1,1′-ferrocenedicarboxylate with other appropriate auxiliary ligands.

2.4. Fluorescence properties

The fluorescence properties of complexes **1–3** and sodium 1,1′-ferrocenedicarboxylate are measured in solid state at room temperature (Fig. 4). The excited wavelengths are all selected at 245 nm, the maximum emission peaks are at 390 nm for **1**, 390 nm for **2**, 392 nm for **3**, 390 nm for sodium 1,1′-ferrocenedicarboxylate and the shoulder peaks at about 289 nm for all of them. Obviously, the fluores-
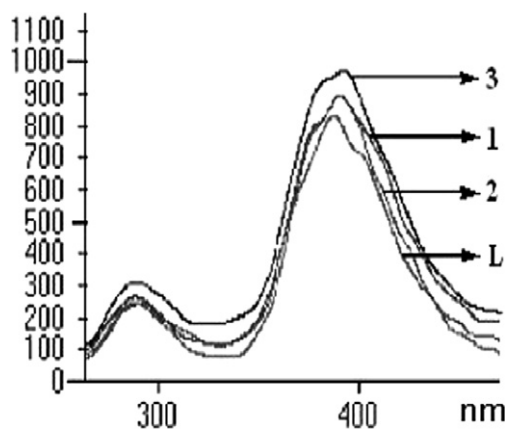

Fig. 4. Emission spectra of sodium 1,1′-ferrocenedicarboxylate (L) and complexes **1–3** in solid state at room temperature.

cence peak positions of complexes **1–3** and sodium 1,1′-ferrocenedicarboxylate are very close, which implies that the fluorescence emissions of **1–3** are ruled by 1,1′-ferrocenedicarboxylate ligand. Therefore, we may suggest that the fluorescence emissions observed in **1–3** can be assigned to the ligand-to-ligand charge transfer (LLCT) emissions. In our previous paper, the fluorescence properties of some 1,1′-ferrocenedicarboxylate complexes have been reported, such as the 2-D layered polymers $\{[M(\eta^2-O_2CFcCO_2-\eta^2)(\mu_2-\eta^2-O_2CFcCO_2-\eta^2-\mu_2)_{0.5}(H_2O)_2] \cdot mH2O\}_n$ (M = Tb^{3+}, Eu^{3+}, Y^{3+}; m = 1 or 2) [17], 1-D wave-shaped polymer $\{[Cd(\eta^2-O_2CFcCO_2-\eta^2)(H_2O)_3] \cdot 4H_2O\}_n$ [17], binuclear complexes $[M_2(\eta^2-O_2CFcCO_2)_2(2,2′-bpy)_2(H_2O)_2]$ (M = Cd; Zn) [19] and $[M_2(O_2CFcCO_2)_2(2,2′-bpy)_2(\mu_2-OH_2)_2]$ (M = Co; Ni) [19]. They give maximum emissions in the range from 390 nm to 393 nm. The fluorescence peak positions of these 1,1′-ferrocenedicarboxylate complexes are near to complexes **1–3** and free sodium 1,1′-ferrocenedicarboxylate. This shows that the fluorescence mechanism of them are similar.

3. Experimental

3.1. General information and materials

All reagents are obtained from commercial suppliers and used as received. IR data are recorded on a BRUKER TENSOR 27 spectrophotometer with KBr pellets in the 400–4000 cm^{-1} region. Elemental analyses (C, H, and N) were carried out on a FLASH EA 1112 elemental analyzer. 1,1′-Ferrocenedicarboxylic acid is prepared according to the literature method [28,29]. Ligands 1,1′-(1,3-propanediyl)bis-1*H*-benzimidazole (prbbm) and 1,1′-(1,5-pentanediyl)bis-1*H*-benzimidazole (pebbm) are prepared according to the literature [30], except that benzimidazole is used instead of benzotriazole.

3.2. Synthesis

3.2.1. Synthesis of $[Cd_2(\eta^2-O_2CFcCO_2-\eta^2)_2(phen)_2(H_2O)_2] \cdot 4CH_3OH$ (**1**)

A methanol-water mixed solution of Fc(CO$_2$Na)$_2$ (0.04 mmol, 3 mL) is added into the 2 mL methanol solution of Cd(NO$_3$)$_2 \cdot 4$H$_2$O (0.02 mmol), then 2 mL methanol solution of phen (0.02 mmol) is added dropwise to the above mixture. The resulting orange solution with pH 5–6 is allowed to stand at room temperature in the dark. Red crystals suitable for X-ray diffraction are obtained after six days. Crystals of complex **1** are stable in the air. Yield: 62%. IR (cm^{-1}, KBr): 3379 m, 3098 w, 1565 s, 1481 s, 1389 s, 1187 m, 1028 m, 804 m, 727 m, 489 m. Anal. Calc. for C$_{52}$H$_{52}$Cd$_2$Fe$_2$N$_4$O$_{14}$: C, 48.28; H, 4.05; N, 4.33. Found: C, 48.64; H, 3.88; N, 4.52%.

Table 1
Crystal data and structure refinement for complexes **1–3**

Complex	**1**	**2**	**3**
Empirical formula	C$_{52}$H$_{52}$Cd$_2$Fe$_2$N$_4$O$_{14}$	C$_{31}$H$_{34}$CdFeN$_4$O$_7$	C$_{29}$H$_{32}$CdFeN$_4$O$_8$
Formula weight	1293.48	742.87	732.84
Temperature (K)	291(2)	291(2)	291(2)
Wavelength (Å)	0.71073	0.71073	0.71073
Crystal system	Triclinic	Triclinic	Monoclinic
Space group	$P\bar{1}$	$P\bar{1}$	$P2_1/n$
Unit cell dimensions			
a (Å)	12.273(6)	11.908(4)	14.347(5)
b (Å)	14.298(7)	12.171(4)	13.994(5)
c (Å)	16.306(8)	13.749(5)	16.509(6)
α (°)	90.811(7)	68.679(4)	90
β (°)	93.089(7)	76.420(4)	98.175(4)
γ (°)	111.470(7)	62.357(4)	90
V (Å^3)	2657(2)	1639.2(10)	3281.2(19)
Z	2	2	4
D_{calc} (g/cm^3)	1.617	1.505	1.484
$F(000)$	1304	756	1488
Crystal sizes (mm)	0.34 × 0.12 × 0.08	0.21 × 0.11 × 0.07	0.36 × 0.30 × 0.05
θ Range (°)	2.75–25.50	2.41–25.50	2.28–27.50
Index ranges	$-14 \leqslant h \leqslant 14, -17 \leqslant k \leqslant 17, -19 \leqslant l \leqslant 19$	$-14 \leqslant h \leqslant 14, -14 \leqslant k \leqslant 14, -16 \leqslant l \leqslant 16$	$-18 \leqslant h \leqslant 18, -18 \leqslant k \leqslant 18, -21 \leqslant l \leqslant 21$
Reflections collected/unique (R_{int})	19127/9553 (0.0833)	12091/5991 (0.0407)	27588/7524 (0.0569)
Data/restraints/parameters	9553/87/675	5991/9/421	7524/78/388
Goodness-of-fit on F^2	1.002	0.977	1.049
Final R indices [$I > 2\sigma(I)$]	$R_1 = 0.0752, wR_2 = 0.1618$	$R_1 = 0.0418, wR_2 = 0.0857$	$R_1 = 0.0518, wR_2 = 0.1583$
R indices (all data)	$R_1 = 0.1603, wR_2 = 0.2042$	$R_1 = 0.0710, wR_2 = 0.0987$	$R_1 = 0.0784, wR_2 = 0.1772$
Largest difference in peak and hole (e Å^{-3})	1.416 and −1.335	0.568 and −0.349	1.206 and −0.620

Table 2
Selected bond lengths (Å) and angles (°) for complexes **1**–**3**

*Complex **1**[a]*
Bond lengths (Å)

Cd(1)–N(1)	2.344(7)	Cd(1)–O(5)	2.331(6)
Cd(1)–N(2)	2.366(8)	Cd(1)–O(1)	2.385(7)
Cd(1)–O(4)#1	2.400(6)	Cd(1)–O(3)#1	2.426(8)
Cd(1)–O(2)	2.474(7)	Cd(2)–N(4)	2.331(8)
Cd(2)–O(10)	2.331(6)	Cd(2)–N(3)	2.361(7)
Cd(2)–O(6)	2.388(7)	Cd(2)–O(8)#2	2.426(8)
Cd(2)–O(7)	2.458(7)	Cd(2)–O(9)#2	2.414(7)
O(3)–Cd(1)#1	2.426(8)	O(4)–Cd(1)#1	2.400(6)
O(8)–Cd(2)#2	2.426(8)	O(9)–Cd(2)#2	2.414(7)

Bond angles (°)

N(1)–Cd(1)–N(2)	71.3(3)	O(5)–Cd(1)–N(2)	170.4(3)
N(1)–Cd(1)–O(1)	133.9(2)	O(5)–Cd(1)–O(1)	90.5(2)
N(2)–Cd(1)–O(1)	95.4(2)	N(1)–Cd(1)–O(4)#1	136.7(3)
O(5)–Cd(1)–O(4)#1	92.5(2)	N(2)–Cd(1)–O(4)#1	95.4(3)
O(1)–Cd(1)–O(4)#1	87.2(2)	N(1)–Cd(1)–O(3)#1	84.3(2)
O(5)–Cd(1)–O(3)#1	87.2(2)	N(2)–Cd(1)–O(3)#1	93.0(3)
O(1)–Cd(1)–O(3)#1	141.5(2)	O(4)#1–Cd(1)–O(3)#1	54.6(2)
N(1)–Cd(1)–O(2)	82.6(2)	O(5)–Cd(1)–O(2)	84.5(2)
N(2)–Cd(1)–O(2)	92.8(2)	O(1)–Cd(1)–O(2)	53.4(2)
O(4)#1–Cd(1)–O(2)	140.3(2)	O(3)#1–Cd(1)–O(2)	163.2(2)
O(10)–Cd(2)–N(4)	100.7(3)	N(4)–Cd(2)–N(3)	71.1(3)
O(10)–Cd(2)–N(3)	171.7(3)	N(4)–Cd(2)–O(6)	133.5(3)
O(10)–Cd(2)–O(6)	91.6(2)	N(3)–Cd(2)–O(6)	93.9(2)
N(4)–Cd(2)–O(8)#2	85.5(3)	O(10)–Cd(2)–O(8)#2	83.8(3)
N(3)–Cd(2)–O(8)#2	95.8(3)	O(6)–Cd(2)–O(8)#2	140.7(3)
N(4)–Cd(2)–O(7)	82.6(3)	O(10)–Cd(2)–O(7)	84.3(2)
N(3)–Cd(2)–O(7)	93.9(3)	O(6)–Cd(2)–O(7)	54.0(2)
O(8)#2–Cd(2)–O(7)	161.3(3)	N(4)–Cd(2)–O(9)#2	135.1(3)
O(10)–Cd(2)–O(9)#2	93.2(2)	N(3)–Cd(2)–O(9)#2	93.2(3)
O(6)–Cd(2)–O(9)#2	87.9(3)	O(9)#2–Cd(2)–O(8)#2	53.6(3)
O(9)#2–Cd(2)–O(7)	141.6(3)		

*Complex **2**[b]*
Bond lengths (Å)

Cd(1)–O(3)#1	2.283(2)	Cd(1)–N(1)	2.300(2)
Cd(1)–N(4)#2	2.353(3)	Cd(1)–O(1)	2.399(3)
Cd(1)–O(5)	2.413(2)	Cd(1)–O(2)	2.498(2)
O(3)–Cd(1)#1	2.283(2)	N(4)–Cd(1)#2	2.353(3)

Bond angles (°)

O(3)#1–Cd(1)–N(1)	131.62(8)	O(3)#1–Cd(1)–N(4)#2	93.83(8)
N(1)–Cd(1)–N(4)#	90.65(8)	O(3)#1–Cd(1)–O(1)	138.66(8)
N(1)–Cd(1)–O(1)	89.01(8)	N(4)#2–Cd(1)–O(1)	92.76(9)
O(3)#1–Cd(1)–O(5)	85.81(7)	N(1)–Cd(1)–O(5)	87.10(8)
N(4)#2–Cd(1)–O(5)	176.63(8)	O(1)–Cd(1)–O(5)	89.71(9)
O(3)#1–Cd(1)–O(2)	85.07(7)	N(1)–Cd(1)–O(2)	141.38(7)
N(4)#2–Cd(1)–O(2)	99.51(8)	O(1)–Cd(1)–O(2)	53.60(7)
O(5)–Cd(1)–O(2)	83.81(8)		

*Complex **3**[c]*
Bond lengths (Å)

Cd(1)–N(1)	2.271(4)	Cd(1)–O(2)	2.295(4)
Cd(1)–N(4)#1	2.310(4)	Cd(1)–O(5)	2.375(3)
Cd(1)–O(3)#2	2.387(4)	Cd(1)–O(4)#2	2.552(4)
Cd(1)–O(1)	2.616(4)	O(3)–Cd(1)#2	2.387(4)
O(4)–Cd(1)#2	2.552(4)	N(4)–Cd(1)#3	2.310(4)

Bond angles (°)

N(1)–Cd(1)–O(2)	136.71(16)	N(1)–Cd(1)–N(4)#1	91.06(16)
O(2)–Cd(1)–N(4)#1	103.76(15)	N(1)–Cd(1)–O(5)	84.76(14)
O(2)–Cd(1)–O(5)	84.92(13)	N(4)#1–Cd(1)–O(5)	170.64(14)
N(1)–Cd(1)–O(3)#2	135.65(16)	O(2)–Cd(1)–O(3)#2	84.56(14)
N(4)#1–Cd(1)–O(3)#2	93.36(14)	O(5)–Cd(1)–O(3)#2	83.89(13)
N(1)–Cd(1)–O(4)#2	84.38(16)	O(2)–Cd(1)–O(4)#2	136.85(14)

Table 2 (*continued*)

N(4)#1–Cd(1)–O(4)#2	83.89(16)	O(5)–Cd(1)–O(4)#2	87.37(14)
O(3)#2–Cd(1)–O(4)#2	52.40(13)	N(1)–Cd(1)–O(1)	87.39(16)
O(2)–Cd(1)–O(1)	52.18(13)	N(4)#1–Cd(1)–O(1)	92.22(15)
O(5)–Cd(1)–O(1)	95.94(14)	O(3)#2–Cd(1)–O(1)	136.39(14)
O(4)#2–Cd(1)–O(1)	170.82(13)		

[a] Symmetry transformations used to generate equivalent atoms in complex **1**: #1: $-x$, $-y$, $-z$; #2: $-x$, $-y+1$, $-z+1$.
[b] Symmetry transformations used to generate equivalent atoms in complex **2**: #1: $-x+2$, $-y+1$, $-z+1$; #2: $-x+1$, $-y+2$, $-z+2$.
[c] Symmetry transformations used to generate equivalent atoms in complex **3**: #1: $-x+3/2$, $y+1/2$, $-z+3/2$; #2: $-x+1$, $-y+1$, $-z+1$; #3: $-x+3/2$, $y-1/2$, $-z+3/2$.

3.2.2. Synthesis of $\{[Cd(\eta^2\text{-}O_2CFcCO_2)\text{-}(pebbm)(H_2O)]\cdot 2H_2O\}_n$ (**2**)

The procedure is similar to that of **1**, except that pebbm is used instead of phen. The resulting orange solution with pH 5–6 is allowed to stand at room temperature in the dark. Orange crystals suitable for X-ray diffraction are obtained after two days. Crystals of complex **2** are stable in the air. Yield: 58%. IR (cm^{-1}, KBr): 3360 m, 3107 m, 2933 m, 1561 s, 1478 s, 1388 s, 1199 m, 1029 m, 803 m, 750 m, 496 m. Anal. Calc. for $C_{31}H_{34}CdFeN_4O_7$: C, 50.12; H, 4.61; N, 7.54. Found: C, 49.86; H, 4.49; N, 7.36%.

3.2.3. Synthesis of $\{[Cd(\eta^2\text{-}O_2CFcCO_2\text{-}\eta^2)(prbbm)(H_2O)]\cdot 3H_2O\}_n$ (**3**)

The procedure is also similar to as that of **1**, except that prbbm is used instead of phen. The resulting orange solution with pH 5–6 is allowed to stand at room temperature in the dark. Orange crystals suitable for X-ray diffraction are obtained after four days. Crystals of complex **3** are stable in the air. Yield: 53%. IR (cm^{-1}, KBr): 3427 m, 3088 w, 1619 m, 1555 s, 1481 s, 1392 m, 1196 m, 1031 m, 804 m, 750 m, 495 m. Anal. Calc. for $C_{29}H_{32}CdFeN_4O_8$: C, 47.53; H, 4.40; N, 7.65. Found: C, 47.87; H, 3.96; N, 7.46%.

3.3. X-ray crystallographic analyses

The data are collected on a Bruker Aper CCD diffractomer with graphite-monochromated Mo Kα radiation ($\lambda = 0.71073$ Å). A single crystal suitable for X-ray diffraction is mounted on a glass fiber. The data are collected at a temperature of 18 ± 1 °C and corrected for Lorenz-polarization effects. A correction for secondary extinction is applied. The structure is solved by direct methods and expanded using Fourier techniques. The non-hydrogen atoms are refined anisotropically and hydrogen atoms are included but not refined. The final cycle of full-matrix least-squares refinement is based on observed reflections and variable parameters. All calculations are performed using the SHELXL-97 crystallographic software package [31], and refined by full-matrix least squares methods based on F^2 with isotropic thermal parameters for the non-hydrogen atoms. Table 1 shows crystallographic crystal data and structure processing parameters of complexes **1**–**3**. Selected bond lengths and bond angles of complexes **1**–**3** are listed in Table 2.

3.4. Determination of fluorescent properties

The luminescent spectra are measured on powder samples at room temperature using a F-4500 HITACHI Fluorescence Spectrophotometer. The excitation slit is 5 nm and the emission slit is 5 nm too, the response time is 2 s.

Appendix A. Supplementary material

Supplementary data associated with this article can be found, in the online version, at doi:10.1016/j.jorganchem.2007.07.001.

References

[1] (a) F.A. Cotton, Z. Li, C.Y. Liu, C.A. Murillo, Inorg. Chem. 6 (2006) 9765;
(b) G.Q. Zhang, G.Q. Yang, J.S. Ma, Cryst. Growth Des. 6 (2006) 1897;
(c) J.J. Perry, G.J. McManus, M.J. Zaworotko, Chem. Commun. (2004) 2534;
(d) B.H. Ye, B.B. Ding, Y.Q. Weng, X.M. Chen, Cryst. Growth Des. 5 (2005) 803;
(e) Z.B. Han, X.N. Cheng, X.M. Chen, Cryst. Growth Des. 5 (2005) 695.
[2] (a) L.R. MacGillivray, J.L. Atwood, Angew. Chem., Int. Ed. 38 (1999) 1018;
(b) A.J. Blake, N.R. Champness, P. Hubberstey, W.S. Li, M.A. Withersby, M. Schröder, Coord. Chem. Rev. 183 (1999) 117;
(c) B.H. Ye, M.L. Tong, X.M. Chen, Coord. Chem. Rev. 249 (2005) 545;
(d) A.N. Khlobystov, A.J. Blake, N.R. Champness, D.A. Lemenovskii, A.G. Majouga, N.V. Zyk, M. Schroder, Coord. Chem. Rev. 222 (2001) 155;
(e) D.F. Sun, D.J. Collins, Y.X. Ke, J.L. Zuo, H.C. Zhou, Chem. Eur. J. 12 (2006) 3768.
[3] (a) D.F. Sun, R. Cao, Y.Q. Sun, W.H. Bi, D.Q. Yuan, Q. Shi, X. Li, Chem. Commun. (2003) 1528;
(b) G.F. Swiegers, T.J. Malefetse, Chem. Rev. 100 (2000) 3483;
(c) H.W. Roesky, M. Andruh, Coord. Chem. Rev. 236 (2003) 91.
[4] (a) B.l. Chen, M. Eddaoudi, S.T. Hyde, M. O'Keeffe, O.M. Yaghi, Science 294 (2001) 1021;
(b) B.J. Holiday, C.A. Mirkin, Angew. Chem., Int. Ed. 40 (2001) 2022;

(c) K.L. Lu, Y.F. Chen, Y.H. Liu, Y.W. Cheng, R.T. Liao, Y.S. Wen, Cryst. Growth Des. 5 (2005) 403;
(d) Y.L. Lu, J.Y. Wu, M.C. Chan, S.M. Huang, C.S. Lin, T.W. Chiu, Y.H. Liu, Y.S. Wen, C.H. Ueng, T.M. Chin, C.H. Hung, K.L. Lu, Inorg. Chem. 45 (2006) 2430.
[5] (a) S.A. Bourne, J.J. Lu, A. Mondal, B. Moultor, M.J. Zaworotko, Angew. Chem., Int. Ed. 40 (2001) 2111;
(b) J.J. Lu, A. Mondal, B. Moultor, M.J. Zaworotko, Angew. Chem., Int. Ed. 40 (2001) 2113;
(c) Y. Cui, O.R. Evans, H.L. Ngo, P.S. White, W.B. Lin, Angew. Chem., Int. Ed. 41 (2002) 1159.
[6] (a) J. Kim, B.L. Chen, T.M. Reineke, H.L. Li, M. Eddaoudi, D.B. Moler, M. O'Keeffe, O.M. Yaghi, J. Am. Chem. Soc. 123 (2001) 8239;
(b) N.L. Rosi, M. Eddaoudi, J. Kim, M. O'Keeffe, O.M. Yaghi, Angew. Chem., Int. Ed. 41 (2002) 284;
(c) H.L. Li, M. Eddaoudi, M. O'Keeffe, O.M. Yaghi, Nature 402 (1999) 276;
(d) J.H. He, J.H. Yu, Y.T. Zhang, Q.H. Pan, R.R. Xu, Inorg. Chem. 44 (2005) 9279.
[7] (a) P.J. Steel, Acc. Chem. Res. 38 (2005) 243;
(b) B. Robert, Eur. J. Inorg. Chem. (2004) 3688.
[8] (a) G.C. Urko, C. Oscar, L. Antonio, G.T. Juan, P.B. Garikoitz, R. Pascual, Cryst. Growth Des. 6 (2006) 1839;
(b) S.A. Barnett, N.R. Champness, Coord. Chem. Rev. 246 (2003) 145;
(c) S.K. Ghosh, J. Ribas, P.K. Bharadwaj, Cryst. Growth Des. 5 (2005) 623;
(d) J.H. Liao, J.S. Juang, Y.C. Lai, Cryst. Growth Des. 6 (2006) 354;
(e) H.L. Sun, B.Q. Ma, S. Gao, S.R. Batten, Cryst. Growth Des. 5 (2005) 1331;
(f) D. Moon, M.S. Lah, Inorg. Chem. 44 (2005) 1934.
[9] (a) P. Børsting, P.J. Steel, Eur. J. Inorg. Chem. (2004) 376;
(b) B. Robert, Inorg. Chim. Acta 357 (2004) 396;
(c) T.L. Hennigar, D.C. MacQuarrie, P. Losier, R.D. Rogers, M.J. Zaworotko, Angew. Chem., Int. Ed. 36 (1997) 972;
(d) B. Moulton, M.J. Zaworotko, Chem. Rev. 101 (2001) 1629;
(e) X.J. Luan, Y.Y. Wang, L.J. Zhou, X.H. Cai, C.H. Zhou, Q.Z. Shi, J. Mol. Struct. 750 (2005) 58;
(f) M.V. Marinho, M.I. Yoshida, K.J. Guedes, K. Krambrock, A.J. Bortoluzzi, M. Hörner, F.C. Machado, W.M. Teles, Inorg. Chem. 43 (2004) 1539;
(g) S.R. Battern, J.C. Jeffery, M.D. Ward, Inorg. Chim. Acta 292 (1999) 231;
(h) L. Carlucci, G. Ciani, D.W.V. Gudenberg, D.M. Proserpio, Inorg. Chem. 36 (1997) 3812;
(i) L. Pan, E.B. Woodloc, X. Wang, K.C. Lam, A.L. Rheingold, Chem. Commun. (2001) 1762;
(j) K. Jin, X. Huang, L. Pang, J. Li, A. Appel, S. Wherland, Chem. Commun. (2002) 2872.
[10] (a) H.W. Hou, L.K. Li, Leading Edge Organometallic Chemistry Research, Nava Science Publishers, Inc., 2006, p. 27;
(b) H.W. Hou, G. Li, L.K. Li, Y. Zhu, X.R. Meng, Y.T. Fan, Inorg. Chem. 42 (2003) 428;
(c) D.W. Slocum, C.R. Ernst, Adv. Organomet. Chem. (1972) 106.
[11] (a) K. Mitsuru, S. Reiko, M. Makoto, M. Khayrul Kabir, I. Yasuhiko, H. Tomonori, N. Tetsuyoshi, M. Kenji, U. Shunji, U. Fumio, J. Chem. Soc., Dalton Trans. (2003) 515;
(b) G.L. Zheng, J.F. Ma, Z.M. Su, L.K. Yan, J. Yang, Y.Y. Li, J.F. Liu, Angew. Chem., Int. Ed. 43 (2004) 2409.
[12] (a) S.M. Lee, K.K. Cheung, W.T. Wong, J. Organomet. Chem. 506 (1996) 77;
(b) J.X. Tao, W.J. Xiao, J. Organomet. Chem. 526 (1996) 21;
(c) W. Uhl, T. Spies, D. Haase, R. Winter, W. Kaim, Organometallics 19 (2000) 1128.
[13] H.W. Hou, X.R. Meng, Y.T. Fan, Y. Zhu, Inorg. Chem. Commun. 9 (2006) 662.
[14] D. Guo, H. Mo, C.Y. Duan, F. Lu, Q.J. Meng, J. Chem. Soc., Dalton Trans. (2002) 2593.
[15] D. Guo, B.G. Zhang, C.Y. Duan, X. Cao, Q.J. Meng, J. Chem. Soc., Dalton Trans. (2003) 282.
[16] (a) Y.Y. Yang, W.T. Wong, Chem. Commun. (2002) 2716;
(b) C. Lopez, R. Costa, F. Illas, E. Molins, E. Espinosa, Inorg. Chem. 39 (2000) 4560;
(c) R. Horikoshi, T. Mochida, H. Moriyama, Inorg. Chem. 41 (2002) 3017;
(d) V.C. Gibson, N.J. Long, A.J.P. White, C.K. Williams, D.J. Williams, Chem. Commun. (2000) 2359.
[17] X.R. Meng, G. Li, H.W. Hou, H.Y. Han, Y.T. Fan, Y. Zhu, C.X. Du, J. Organomet. Chem. 679 (2003) 153.
[18] S.D. Christie, S. Subramanian, L.K. Thompson, M.J. Zaworotko, J. Chem. Soc., Chem. Commun. (1994) 2563.
[19] X.R. Meng, H.W. Hou, G. Li, B.X. Ye, T.Z. Ge, Y.T. Fan, Y. Zhu, H. Sakiyama, J. Organomet. Chem. 689 (2004) 1218.
[20] T.A. Zevaco, H. Corls, E. Dinjus, Polyhedron 17 (1998) 613.
[21] D. Guo, Y.T. Li, C.Y. Duan, H. Mo, Q.J. Meng, Inorg. Chem. 42 (2003) 2519.
[22] S.W. Leng, G. Wu, M.H. Xin, L.L. Tang, G.S. Zhu, Y. Gan, S.H. Shi, GaoDengXueXiaoHuaXueXueBao 25 (2004) 817.
[23] L.L. Wen, B.G. Zhang, Z.H. Peng, J.G. Ren, P. Cai, C.Y. Duan, WuJiHuaXueXueBao 19 (2003) 34.
[24] J. Yang, J.F. Ma, Y.Y. Liu, S.L. Li, G.L. Zheng, Eur. J. Inorg. Chem. 2005 (2005) 2174.
[25] S.L. Zheng, J.H. Yang, X.L. Yu, X.M. Chen, W.T. Wong, Inorg. Chem. 43 (2004) 830.
[26] X.L. Zhang, X.M. Chen, Cryst. Growth Des. 5 (2005) 617.
[27] H.B. Xu, Z.M. Su, K.Z. Shao, Y.H. Zhao, Y. Xing, Y.C. Liang, H.J. Zhang, D.X. Zhu, Inorg. Chem. Commun. (2004) 260.
[28] M.D. Rausch, D.J. Ciappenelli, J. Organomet. Chem. 10 (1967) 127.
[29] (a) Gmelin Handbuch der Anorganische Chemie. Eisen Organische Verbindungen, vol. A3, Springer, Berlin, Germany, 1976, p. 58;
(b) A. Slawisch, Gmelin Handbuch der Anorganischen Chemie, vol. 8, Springer, Berlin, 1986, p. 210.
[30] X.J. Xie, G.S. Yang, L. Cheng, F. Wang, Huaxue Shiji 22 (2000) 222.
[31] G.M. Sheldrick, SHELXL-97: Program for Refinement of Crystal Structure, University of Göttingen, Göttingen, Germany, 1997.